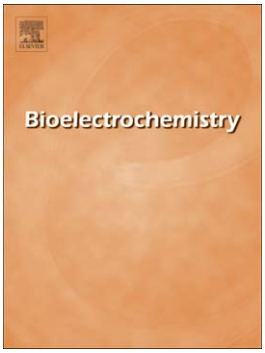

A new self-assembled layer-by-layer glucose biosensor based on chitosan biopolymer entrapped enzyme with nitrogen doped graphene

Madalina M. Barsan, Melinda David, Monica Florescu, Laura Ţugulea, Christopher M.A. Brett

PII: S1567-5394(14)00086-3
DOI: doi: 10.1016/j.bioelechem.2014.06.004
Reference: BIOJEC 6751

To appear in: *Bioelectrochemistry*

Received date: 18 March 2014
Revised date: 13 June 2014
Accepted date: 13 June 2014

Please cite this article as: Madalina M. Barsan, Melinda David, Monica Florescu, Laura Ţugulea, Christopher M.A. Brett, A new self-assembled layer-by-layer glucose biosensor based on chitosan biopolymer entrapped enzyme with nitrogen doped graphene, *Bioelectrochemistry* (2014), doi: 10.1016/j.bioelechem.2014.06.004

A new self-assembled layer-by-layer glucose biosensor based on chitosan biopolymer entrapped enzyme with nitrogen doped graphene

Madalina M. Barsan[1], Melinda David[1,2], Monica Florescu[3], Laura Ţugulea[2], Christopher M.A. Brett[1,*]

[1]*Departamento de Química, Faculdade de Ciências e Tecnologia, Universidade de Coimbra, 3004-535 Coimbra, Portugal*
[2]*Facultatea de Fizica, Universitatea din Bucuresti, Magurele 077125, Romania*
[3]*Facultatea de Medicina, Universitatea Transilvania din Brasov, Brasov 500019, Romania*

* Corresponding author:
Tel: +351-239854470
FAX: +351-239827703
E-mail: cbrett@ci.uc.pt

Abstract

The layer-by-layer (LbL) technique has been used for the construction of a new enzyme biosensor. Multilayer films containing glucose oxidase, GOx, and nitrogen-doped graphene (NG) dispersed in the biocompatible positively-charged polymer chitosan ($chit^+$(NG+GOx)), together with the negatively charged polymer poly(styrene sulfonate), PSS^-, were assembled by alternately immersing a gold electrode substrate in $chit^+$(NG+GOx) and PSS^- solutions. Gravimetric monitoring during LbL assembly by an electrochemical quartz microbalance enabled investigation of the adsorption mechanism and deposited mass for each monolayer. Cyclic voltammetry and electrochemical impedance spectroscopy were used to characterize the LbL modified electrodes, in order to establish the contribution of each monolayer to the overall electrochemical properties of the biosensor. The importance of NG in the biosensor architecture was evaluated by undertaking a comparative study without NG in the chit layer. The GOx biosensor's analytical properties were evaluated by fixed potential chronoamperometry and compared with similar reported biosensors. The biosensor operates at a low potential of -0.2 V vs., Ag/AgCl, exhibiting a high sensitivity of 10.5 µA cm^{-2} mM^{-1}, and a detection limit of 64 µM. This study shows a simple approach to developing new biosensor architectures, combining the advantages of nitrogen-doped graphene with the LbL technique for enzyme immobilization.

Keywords: layer-by layer; quartz crystal microbalance; nitrogen doped graphene; enzyme; chitosan

1. Introduction

One of the key issues in developing new biosensors with improved sensitivity and stability is effective immobilization of the recognition element, e.g. the enzyme. Among the enzyme immobilization methods, such as covalent linkage [1,2], sol-gel entrapment [3,4], adsorption [5], etc., layer-by-layer (LbL) self-assembly is a simple and powerful method, efficient because protein denaturation is minimised since the films are produced under mild conditions, based on the adsorption of macromolecules from aqueous solution onto solid supports [6]. LbL films have unique mechanical properties, uniformity and stability [7], the technique having the advantage of allowing the construction of thin multilayer films, based mainly on electrostatic interactions in between layers, which require a very small amount of material, therefore being a cost-effective preparation method for enzyme biosensors.

One of the problems to be overcome in an enzyme biosensor is the slow electron transfer between the enzyme redox centre, which is usually buried in a hydrophobic cavity formed by polypeptide, and the electrode surface. Nanomaterials, such as graphene, carbon nanotubes (CNTs), metal nanoparticles, etc., are advantageous in increasing the possibility of direct electron transfer between the enzyme active sites and the electrode, acting as electrical bridges [8-10]; however, direct electron transfer between enzymes and carbon nanomaterials is not always the mechanistic basis of the substrate detection [11]. Nanomaterials can also bring benefits for immobilizing enzymes since they maintain enzyme bioactivity due to their microenvironment [12, 13]. Among the above-mentioned materials, graphene is a 2D plane sheet with an open structure and both sides of graphene could be utilized for enzyme immobilization, unlike 1-D CNTs, which are more difficult to be controllably assembled [14]. LbL formation of multilayer films with incorporation of graphene in one of the components of the self-assembly process combines the excellent electrochemical properties of graphene and the versatility of LbL assembly, showing great promise for highly efficient sensors and advanced biosensing systems. The excellent conductivity and small band gap of graphene are favourable for conducting electrons from the biomolecules [15]. Although, by using different types of intermolecular interactions, LbL structures are able to incorporate diverse molecules as building blocks, it is still a challenge to include certain kinds of molecules, especially hydrophobic species, into LbL films [16].

Graphene and nitrogen-doped graphene (NG) have been successfully dispersed in chitosan and used as substrate for the immobilization of enzymes [9, 17]. The N-doping of graphene has been done by thermal annealing in the presence of ammonia, the nitrogen atom in the graphene framework existing in “graphitic”, pyridinic or pyrrolic forms, which are beneficial for the electric conductivity of the material [18]. The biopolymer chitosan (chit) is often employed for enzyme immobilization, through covalent linkage, when the polymer is chemically modified to allow crosslinking with enzyme aminoacids [19], and by electrostatic interaction in LbL films [20], in this case usually combined with carbon nanotubes, redox mediators or metal nanoparticles, due to its relatively poor conductivity [10, 21].

In the LbL enzyme immobilization study presented here, the positively-charged chitosan layer contains the enzyme glucose oxidase (GOx) together with dispersed NG, $chit^{+}$(GOx) or $chit^{+}$(NG+GOx), and the negatively charged layer is poly(styrene sulfonate), PSS^{-}. Self-assembled adsorption of the multilayers on Au substrates was monitored by using an electrochemical quartz crystal microbalance (EQCM), cyclic voltammetry (CV) and electrochemical impedance spectroscopy (EIS). The influence of NG and of each monolayer on the electrochemical properties of the LbL biosensor was analysed, together with biosensor sensitivity after addition of each enzyme layer, in order to determine the best biosensor architecture.

2. Experimental

2.1 Reagents and solutions

All reagents were of analytical grade and were used without further purification. N-doped graphene was prepared according to the procedure described in [18] and was a gift from Prof. X. Sun, University of Western Ontario, Canada. Chitosan (low molecular weight), minimum 85% degree of deacetylation, monobasic and dibasic sodium phosphate, and sodium polystyrene sulfonate (NaPSS) were from Sigma-Aldrich, Germany. The deacetylated chitosan used in this study was chosen due to its higher positive charge density. Glucose oxidase (GOx) from *Aspergillus niger* (24 U mg^{-1}) was from Fluka, Germany.
Experiments were performed in neutral sodium phosphate buffer 0.1 M NaPB pH=7.0. Millipore Milli-Q nanopure water (resistivity ≥ 18 MΩ cm) was used for the preparation of all solutions. All experiments were performed at room temperature (25±1 °C).

2.2 Instrumentation

Gravimetric measurements were performed with an electrochemical quartz crystal microbalance eQCM 10 M, Gamry Instruments, containing an Au quartz crystal (AuQC) with 10 MHz central frequency.
Electrochemical experiments were performed in a three-electrode cell, containing the AuQC (area 0.205 cm^2) as working electrode, a Pt wire counter electrode and an Ag/AgCl (3.0 M KCl) reference electrode, using a µ-Autolab potentiostat/galvanostat (Metrohm-Autolab, Netherlands).
Electrochemical impedance spectroscopy (EIS) experiments were carried out with a potentiostat/galvanostat/ZRA, (Gamry Instruments, Reference 600). An rms perturbation of 10 mV was applied over the frequency range 65 kHz–0.1 Hz, with 10 frequency values per frequency decade.
The pH measurements were carried out with a CRISON 2001 micro pH-meter (Crison Instruments SA, Barcelona, Spain) at room temperature (25±1ºC).

2.3. Preparation of the LbL biosensors

NG was used as received and was dispersed together with the enzyme GOx in 1% (w/v) chitosan dissolved in 1% (v/v) acetic acid, to obtain a final solution containing 0.05% NG and 1% GOx (24 U in 100 µL of enzyme solution). This solution had a pH of 4.0, just below the isoelectric point of GOx, which is 4.2 [22], so that both chitosan and enzyme were positively charged. The AuQC was always previously cleaned with acetone and placed in the AuQCM cell, which is a small chamber of 200 µL liquid capacity with the AuQC on the cell bottom and into which the counter and reference electrodes are inserted. For the gravimetric studies, 200 µL of water was first placed in the chamber by micropipette to allow the stabilization of frequency in aqueous media. Then the water was removed and 200 µL of the solution containing the NG+GOx or GOx, i.e. $chit^+$(NG+GOx)) or $chit^+$(GOx) was placed in the chamber and left for 60 min, followed by rinsing with water and drying with a nitrogen stream, during 2-3 min. Following this, the chamber was filled with 200 µL of negatively charged 1% NaPSS solution and left during 20 min, then again rinsed with water and dried with a nitrogen stream, during 2-3 min. This procedure was repeated for further bilayers In this way, biosensors AuQC/{$chit^+$(NG+GOx)/PSS^-/$chit^+$(NG+GOx)}$_n$ (n=1, 2) or AuQC/{$chit^+$(GOx)/PSS^-/$chit^+$(GOx)}$_n$ (n=1, 2) were obtained.

3. Results and discussion

3.1. Gravimetric monitoring of the chit$^+$(NG+GOx)/PSS$^-$ and chit$^+$(GOx)/PSS$^-$ self-assembly on AuQC

The QCM is an excellent tool of monitoring the dynamics of the adsorption process during LbL self-assembly. The frequency variation with time can be used to determine the deposited mass by using the Sauerbrey equation [23], for the specific case of rigid films:

$$\Delta f = -\frac{2 f_0^2}{A\sqrt{\mu_q \rho_q}} \Delta m$$

where f_0 is the resonant frequency (Hz), Δf the frequency change (Hz), Δm the mass change (g), A the piezoelectrically active crystal area, ρ_q the density of quartz (g cm^{-3}) and μ_q the shear modulus of quartz for AT-cut crystals (g cm^{-1} s^{-2}). In the specific case of the AuQCM employed in this study, the conversion factor, $-\Delta f / \Delta m$, is 226.0 Hz per 1 µg.
The AuQCM cell utilized is a small chamber of capacity 200 µL of liquid. Water was first placed in the chamber in order to stabilize the crystal resonant frequency in liquid, was emptied by using a micropipette, and dried with a nitrogen stream. Self-assembly then began with chit$^+$(NG+GOx) solution as described in Section 2.3.
As shown in Fig. 1A, red line, the AuQC frequency immediately decreased when it contacted for the first time with the chit$^+$(NG+GOx) solution, indicating fast adsorption of the molecules on the clean AuQC surface. The overall shift in frequency for this first step was Δf_1 = 0.93 kHz, corresponding to a deposited mass of m_1 = 850 ng. The deposition vs. time profile of PSS$^-$ followed an exponential decrease, of Δf_2 = 3.41 kHz, a film of m_2 = 2.06 µg being deposited. An exponential decrease in frequency was also observed for the second immersion of the AuQC in the chit$^+$(NG+GOx) solution Δf_3 = 8.45 kHz, with a fast and sharp decay during the first 30 min, of 7.96 kHz, and a slower for the next 30 min, corresponding to 1.30 kHz. This indicates that fast adsorption of molecules occurs in the first 30 min, the film formed being of mass 7.26 µg, only 1.19 µg being deposited afterwards.
The total decrease in frequency was Δf_{tot} = 13.61 kHz, corresponding to a deposited film of m_{tot} = 12.36 µg.

Here Fig. 1

A AuQCM/{chit$^+$(GOx)/PSS$^-$/chit$^+$(GOx)} was also constructed, this time the chitosan solution containing only the enzyme GOx, without dispersed NG. The frequency and mass shift during the LbL process is presented in Fig.1 (A) and (B), blue line. As can be observed, the deposition profile during the first two self-assembly steps is similar to that obtained for AuQCM/{chit$^+$(NG+GOx)/PSS$^-$/chit$^+$(NG+GOx)}, but there is a significant difference in the last LbL deposition step, when only a small shift in frequency is recorded when NG is not present. The shift in frequency for the first step was Δf_1 = 1.21 kHz, m_1 = 1.11 µg, for the second one Δf_2 = 4.49 kHz, m_2 = 4.06 µg and of the last only Δf_3 = 0.73 kHz, m_3 = 0.76 µg. The fact that only for the third layer is the deposited mass considerably different, i.e. 0.76 and 8.45 µg, without and with NG respectively, indicates that during this step it is mainly NG that is deposited, and that during the first chit$^+$(GOx) or chit$^+$(NG+GOx) adsorption step mainly enzyme is adsorbed. The total deposited mass was m_{tot} = 5.92 µg, which, assuming that chitosan and enzyme adsorb equally, corresponds to 0.07 units of enzyme. The mass is more

than a factor of two lower than that recorded at AuQCM/{chit$^+$(NG+GOx)/PSS$^-$ /chit$^+$(NG+GOx)}, m_{tot} 12.36 µg. A likely explanation for this, taking into account the nanoscale size of NG, is that, besides adsorption of NG, absorption of NG into the previously deposited layers also occurs, leading to incorporation of more NG.

3.2. Cyclic voltammetry and electrochemical impedance spectroscopy characterization of the modified AuQC-s

3.2.1 Cyclic voltammetry (CV)

Cyclic voltammograms were recorded at AuQC, AuQC/chit$^+$(NG+GOx) and AuQC/chit$^+$(NG+GOx) /PSS$^-$/chit$^+$(NG+GOx) in 0.1 M NaPB pH 7.0 (see Fig. 2 (A)). As can be seen, the first layer of chit$^+$(GOx+NG) leads to a substantial increase in the capacitive current, which then decreases slightly for the second chit$^+$(GOx+NG) layer.
CV-s were also recorded at AuQC electrodes modified with chitosan solution containing only the enzyme GOx, without NG, i.e. AuQC/chit$^+$(GOx) and AuQC/chit$^+$(GOx)/PSS$^-$ /chit$^+$(GOx), respectively, in order to evaluate the influence of the NG on the overall electrochemical properties (see Fig. 2 (B)). In this case, the capacitive current decreased continuously for the AuQC modified with the first and second layer of adsorbed chit$^+$(GOx), due to the diffusion barrier caused by the chitosan layer, which without added NG has poor conductivity [21]. In the case of chit$^+$(GOx+NG), the presence of NG leads to an increase in the chitosan layer conductance, but its resistive character is seen when the second layer is adsorbed (see CV at AuQC/AuQC/chit$^+$(NG+GOx)/PSS$^-$/chit$^+$(NG+GOx)), which leads to a slight decrease of the capacitive current due to the first layer. These results clearly demonstrate the importance of using NG dispersed in the chitosan layer, together with the enzyme. Moreover, it was observed that addition of a third layer of chit$^+$(NG+GOx), leads to a more drastic decrease of the capacitive current (results not shown).

Here Fig. 2

The capacitance values were calculated from the CV-s displayed in Fig. 2 (A) and (B), in the potential region close to 0.0 V, where no faradaic reaction occurred. When the chitosan contained NG, there is a significant increase in the capacitance value from 59.6 µF cm^{-2}, on bare AuQC to 341 µF cm^{-2} for the first layer of chit$^+$(NG+GOx), followed by a decrease to 245 µF cm^{-2}, for the second deposited layer. On the other hand, in the absence of NG in the chit layer, the capacitance value decreases continuously with each chit$^+$(GOx) layer, from 58.6 µF cm^{-2}, for bare AuQC to 43.6 and 40.4 µF cm^{-2}, for the first and second deposited chit$^+$(GOx) layer respectively.
CV-s at AuQC/chit$^+$(NG+GOx)/PSS$^-$ and AuQC/chit$^+$(GOx)$^+$/PSS$^-$ were also recorded, and it was observed that the PSS$^-$ layer did not change the CV profile of the AuQC/chit$^+$(NG+GOx) or AuQC/chit$^+$(GOx) (results not shown). This indicates that PSS$^-$ acts only as a conducting layer and it is thin enough not to constitute an additional diffusion barrier in the biosensor architecture.

3.2.2. Electrochemical impedance spectroscopy (EIS)

Electrochemical impedance spectroscopy was employed to evaluate the electrical properties of the LbL biosensors, AuQC/chit$^+$(NG+GOx)/PSS$^-$/chit$^+$(NG+GOx) and AuQC/chit$^+$(GOx)/PSS$^-$/chit$^+$(GOx).

As observed from Fig. 3 (A), adsorptive deposition of the first layer of chit$^+$(NG+GOx), leads to a significant decrease of the impedance values and radius of the second semicircle, which then increases after deposition of the second layer. This is in agreement with what was observed by CV and also, in accordance with the CV-s, PSS^- did not influence the spectra of AuQC/chit$^+$(NG+GOx). On the contrary, see Fig.3 (B), in the absence of NG, each addition of chit$^+$(GOx) lead to an increase in the semicircle radius, indicating an increase in the charge transfer resistance values.
The spectra were fitted to the electrical equivalent circuit shown in Fig. 3 (C), which consists of a cell resistance, R_Ω, in series with a combination of a charge transfer resistance, R_{ct}, in parallel with a double layer constant phase element (CPE_{dl}). The spectra recorded at AuQC/chit$^+$(NG+GOx) AuQC/chit$^+$(NG+GOx)/PSS^-/chit$^+$(NG+GOx) presented an additional small semicircle in the high frequency region, attributed to the NG-containing chitosan film, fitted by another parallel combination of film resistance, R_f, and film CPE, CPE_f. The CPE element was modelled as a non-ideal capacitor, given by $CPE = ((i\omega C)^{\alpha})^{-1}$ where C is the capacitance, ω is the radial frequency in rad s^{-1} and the exponent α reflects the surface non-uniformity and film porosity, having a maximum value of 1.0 and minimum of 0.5 [24].

Here Fig. 3

The data obtained by fitting the spectra are presented in Table 1 A and B. Two different bare AuQC were used as substrates, so that slightly different spectra and therefore parameters were obtained. Regarding the interface with electrolyte solution, represented by R_{ct} in parallel with CPE_{dl}, the charge transfer resistance decreased substantially from 86.9 on AuQC, to 8.6 kΩ cm^2, for the first chit$^+$(NG+GOx) layer, increasing afterwards to 23.2 kΩ cm^2, with the adsorption of a second chit$^+$, meaning that charge transfer is fastest at AuQC/chit$^+$(NG+GOx), and then hindered slightly by the addition of a new layer, due to the resistive effect of chitosan [17]. The CPE_{dl} value increased first from 18.6 to 346 μF cm^{-2} $s^{\alpha-1}$, due to an increase in charge separation, and consequently decreased to 128 μF cm^{-2} $s^{\alpha-1}$ with increase in the R_{ct} value. The α_1 value was almost equal after deposition of the first and second layers of GOx, indicating that the surface homogeneity and uniformity is the same.
An additional high frequency semicircle was recorded at chit$^+$(NG+GOx) modified AuQC, seen in Fig 3 (A) magnification, which was attributed to the electrical properties of the multilayer film. As observed in Table 1, the R_f values of 17.8 and 46.3 Ω cm^2 are much lower than the R_{ct} values, higher for the thicker film containing two chit$^+$(NG+GOx) layers. The CPE_f values were also higher than the CPE_{dl} values, this being attributed to the capacitive properties of NG, being of 1.24 and 0.413 mF cm^{-2} $s^{\alpha-1}$, for the chit$^+$(NG+GOx) and chit$^+$(NG+GOx)/PSS^-/chit$^+$(NG+GOx) respectively. The α_2 values were smaller than the α_1 values, due to the non-uniformity and porosity of the chit$^+$(NG+GOx) film itself.

Here Table 1

The data corresponding to the LbL modified electrode obtained without NG in the chit$^+$(GOx) layers, are also included in Table 1. As expected from the impedance spectra, R_{ct} values increase slightly with each chit$^+$(GOx) layer, from 52.1 to 65.6 and 86.7 kΩ cm^2, respectively, with a corresponding decrease of the CPE_{dl} values from 21.1 μF cm^{-2} $s^{\alpha-1}$, for the bare AuQC to 15.6 μF cm^{-2} $s^{\alpha-1}$, being the same for the first and second chit$^+$(GOx) layer.
A similar effect of chitosan and graphene was reported in [17], in which an increase in the R_{ct} value after direct drop-casting of chitosan on bare glassy carbon electrodes was observed, but in the presence of graphene in the chitosan layer, the R_{ct} value became lower.

In conclusion, the presence of N-doped graphene decreases the charge transfer resistance of the assembly, increasing the interfacial capacitance and provides a film matrix that presents significant charge separation.

3.3. Analytical parameters of the newly developed biosensor and comparison with literature

The AuQC/chit^{+}(NG+GOx)/PSS^{-}/chit^{+}(NG+GOx) biosensor was tested for the detection of glucose by fixed potential chronoamperometry. A typical chronoamperogram at -0.2 V vs. SCE is shown in Fig. 4 (A), with the corresponding calibration plot in Fig. 4 (B). The applied potential in the chronoamperometric measurements was chosen taking into account previous work on GOx biosensors [25]. The response of the biosensor was tested at -0.3, -0.2 and -0.1 V vs. Ag/AgCl, -0.4 V being excluded since it is very close to the hydrogen evolution potential at Au electrodes. At -0.1 V the response was very weak, and since no significant differences in biosensor response were obtained at -0.3 and -0.2 V (a slight decrease from 11.1 to 10.5 μA cm^{-2} mM^{-1}), the value of -0.2 V vs. Ag/AgCl was chosen, in order to minimize the effect of interferents.

The biosensor response was linear between 0.2 and 1.8 mM, with a sensitivity of 10.5 ± 0.9 (8.6 %) μA cm^{-2} mM^{-1} and the detection limit, calculated as 3 times standard deviation divided by slope, was 64 μM, calculated as (3*standard deviation)/sensitivity [26]. The AuQC/chit^{+}(GOx)/PSS^{-}/chit^{+}(GOx) biosensor was also evaluated and, as expected, had a lower sensitivity of only 0.8 μA cm^{-2} mM^{-1}, and a detection limit of 112 μM. The addition of a third and fourth layer does not bring further improvement in biosensor sensitivity, actually decreasing it, due to the resistive nature of chitosan and probably also due to diffusion barriers in between the layers

Here Fig. 4

Since O_2 can both influence enzyme activity and can be involved in the enzymatic reaction mechanism, the influence of oxygen on biosensor performance was analysed by recording fixed potential chronamperograms in buffer solution without oxygen (saturated with N_2) and with normal oxygen content. The results showed that the sensitivity of the biosensor is approximately one half in deoxygenated buffer (from 10.5 down to 6.0 μA cm^{-2} mM^{-1}).
If O_2 is involved in the mechanism forming H_2O_2, as the electron acceptor from $FADH_2$, then at a potential of -0.2 V vs. Ag/AgCl the reduction of generated H_2O_2 is expected to occur. Since the currents recorded were always oxidation currents, and the removal of O_2 did not lead to an increase in the biosensor response, it can be deduced that the mechanism involves direct regeneration of $FADH_2$. The fact that the GOx biosensor sensitivity is lower in deoxygenated buffer is supported by the fact that enzyme activity is highest when O_2 is present, since the GOx is from the highly aerobic species *Aspergillus Niger*."
The AuQC/chit^{+}(NG+GOx)/PSS^{-}/chit^{+}(NG+GOx) stability was evaluated by recording one calibration plot every day during two weeks, and the stability maintained 95% of its initial value, pointing out an excellent conservation of both enzyme amount in the layer by layer structure and enzyme initial activity.
The effect of some electroactive compounds on the biosensor response to glucose was also performed, by first injecting 0.3 mM glucose, followed by injection of 0.6 mM of the interferent solutions (ratio 1:2): ascorbate, uric acid, dopamine, citric acid, oxalic acid, fructose and catechol. No oxidation or reduction currents were recorded after injection of any

of these compounds and the response to glucose in the presence of interferents in these conditions suffered a maximum reduction of 2 %.
In Table 2, analytical parameters of some recent biosensors containing similar components to that developed in the present study are summarised.

Here Table 2

The present biosensor operates at a potential of -0.2 V vs. Ag/AgCl, lower than most of those reported in Table 2. The sensitivity is higher than those reported in [21,27,29,30], the biosensors with higher sensitivities in [10,17,28, 31-34] requiring a higher overpotential, except for the one reported in [10], which operated at the same potential. In [10], the immobilization methods used involved the direct deposition of a greater amount of enzyme and a large amount of MWCNT. Cross-linking with glutaraldehyde led to 0.1 mg enzyme (corresponding to 2 U) to be placed on the electrode and drop casting of the MWCNT dispersion corresponded to 0.2 mg MWCNT being deposited. So the higher sensitivity of the biosensor reported in [10] can be attributed to more units of immobilized enzyme in the biosensor architecture.

4. Conclusions

Biosensors based on LbL self-assembly of the positively charged polymer chitosan, containing the enzyme glucose oxidase and nitrogen-doped graphene, with the negatively charged poly(styrene sulfonate), AuQC/{chit$^+$(NG+GOx)/PSS$^-$/chit$^+$(NG+GOx)}$_n$ (n=1, 2) or AuQC/{chit$^+$(GOx)/PSS$^-$/chit$^+$(GOx)}$_n$ (n=1, 2), have been successfully constructed. A quartz crystal microbalance gravimetric study showed that the total shift in frequency at AuQC/chit$^+$(NG+GOx)/PSS$^-$/chit$^+$(NG+GOx) was 13.61 kHz corresponding to a deposited film of 12.36 µg, being more than twice lower in the absence of NG.
Cyclic voltammetry showed that the first layer of chit$^+$(GOx+NG) leads to a substantial increase in the capacitive current, which then decreased slightly for the second chit$^+$(GOx+NG) layer. When NG was not present in the chit layer, the capacitive current decreased continuously for the AuQC modified with the first and second layer of adsorbed chit$^+$(GOx), underlying the importance of NG in the biosensor architecture. This deduction was reinforced by the EIS results, which indicate that the chit$^+$(NG+GOx) modified electrodes present higher capacitance values and lower charge transfer resistance values than those modified with chit$^+$(GOx).
The biosensor operates at a potential of -0.2 V vs. Ag/AgCl, i.e. close to zero, which is important for reducing the effect of interferents, and has a sensitivity higher than other biosensors operating at close to -0.2 V.
The results demonstrate the advantage of preparing biosensors using nitrogen doped graphene together with the LbL technique, for the immobilization of enzymes that uses less reagents and can lead to more efficient sensor operation. This approach can be extended to other carbon nanomaterials, such as carbon nanotubes, fullerenes, carbon nanorods/nanohorns etc. with enzymes.

Acknowledgements

Financial support from Fundação para a Ciência e a Tecnologia (FCT), Portugal PTDC/QUI-QUI/116091/2009, POCH, POFC-QREN (co-financed by FSE and European Community FEDER funds through the program COMPETE – Programa Operacional Factores de Competitividade under the projects PEst-C/EME/UI0285/2013) and CENTRO -07-0224 -

FEDER -002001 (MT4MOBI)) is gratefully acknowledged. M.M.B. thanks FCT for a postdoctoral fellowship SFRH/BPD/72656/2010 and M.D. thanks the European Commission for a grant under the Erasmus student exchange programme. The authors thank Prof. X. Sun, University of Western Ontario for the gift of N-doped graphene.

References

[1] R.A. Sheldon, R. Schoevaart, L. van Langen, A novel method for enzyme immobilization, Biocat. Biotrans 23 (2005) 141-147.

[2] M.E. Ghica, C.M.A. Brett, A glucose biosensor using methyl viologen redox mediator on carbon film electrodes, Anal. Chim. Acta 532 (2005) 145-151.

[3] R. Pauliukaite, M. Schoenleber, P. Vadgama C.M.A. Brett, Development of electrochemical biosensors based on sol-gel enzyme encapsulation and protective polymer membranes, Anal. Bioanal. Chem., 390 (2008) 1121-1131.

[4] M. Florescu, M. Barsan, R. Pauliukaite, C.M.A. Brett, Development and application of oxysilane sol–gel electrochemical glucose biosensors based on cobalt hexacyanoferrate modified carbon film electrodes, Electroanalysis 19 (2007) 220-226.

[5] M.D. Trevan, Enzyme immobilization by adsorption, Methods Mol. Biol. 3 (1988) 481-489.

[6] M. Campas, C. O'Sullivan, Layer-by-Layer biomolecular assemblies for enzyme sensors, immunosensing, and nanoarchitectures, Anal. Lett. 36 (2003) 2551-2569.

[7] L.G. Paterno, M.A.G. Soler, Layer-by-layer enabled nanomaterials for chemical sensing and energy conversion, JOM, Vol. 65 (2013), 709-719.

[8] B.P. López, A. Merkoçi, Nanomaterials based biosensors for food analysis applications, Trends Food Sci. Technol. 22 (2011) 625-639.

[9] K.P. Prathish, M.M. Barsan, D. Geng, X. Sun, C.M.A. Brett, Chemically modified graphene and nitrogen-doped graphene: electrochemical characterisation and sensing applications, Electrochim. Acta 114 (2013) 533-542.

[10] M.E. Ghica. R. Pauliukaite, O. Fatibello-Filho, C.M.A. Brett, Application of functionalised carbon nanotubes immobilised into chitosan films in amperometric enzyme biosensors Sens. Actuators B 142 (2009) 308-315.

[11] M. Wooten, S. Karra, M. Zhang, W. Gorski, On the direct electron transfer, sensing, and enzyme activity in the glucose oxidase/carbon nanotubes system, Anal. Chem. 86 (2014) 752−757.

[12] K. Balasubramanian, M. Burghard, Biosensors based on carbon nanotubes, Anal. Biochem. 385 (2006) 452-468.

[13] T.T. Baby, S. Aravind, T. Arockiadoss, R. Rakhi, S. Ramaprabhu, Metal decorated graphene nanosheets as immobilization matrix for amperometric glucose biosensor, Sens. Actuators B 145 (2010) 71-77.

[14] W. Yang, K.R. Ratinac, S.P. Ringer, P. Thordarson, J.J. Gooding, F. Braet, Carbon nanomaterials in biosensors: should you use nanotubes or graphene?, Angew. Chem. Int. Ed., 49 (2010) 2114-2138.

[15] S. Stankovich, D.A. Dikin, G.H.B. Dommett, K.M. Kohlhaas, E.J. Zimney, E.A. Stach, R.D. Piner, S.T. Nguyen, R.S. Ruoff, Graphene-based composite materials, Nature 442 (2006) 282-286.

[16] Y.M. Guo, W. Geng, J.Q. Sun, Layer-by-layer deposition of polyelectrolyte-polyelectrolyte complexes for multilayer film fabrication, Langmuir 25 (2009) 1004-1010.

[17] X. Kang, J. Wang, H. Wu, I.A. Aksay, J. Liu, Y. Lin, Glucose Oxidase‑graphene‑chitosan modified electrode for direct electrochemistry and glucose sensing, Biosensors and Bioelectronics 25 (2009) 901-905.

[18] D. Geng, S. Yang, Y. Zhang, J. Yana, J. Liu, R. Li, T.-K.Sham, X. Sun, S. Ye, S. Knights, Nitrogen doping effects on the structure of graphene, Appl. Surf. Sci. 257 (2011) 9193-9198

[19] M. Zhang, C. Mullens, W. Gorski, Chitosan-glutamate oxidase gels: synthesis, characterization, and glutamate determination. Electroanalysis 17, 2005, 2114-2120.
[20] L. Caseli, D.S. dos Santos Jr., M. Foschini, D. Gonçalves, O.N. Oliveira Jr. The effect of the layer structure on the activity of immobilized enzymes in ultrathin films, J. Colloid Interface Sci. 303 (2006) 326-331.
[21] Y. Zou, C. Xiang, L. Sun, F. Xu, Amperometric glucose biosensor prepared with biocompatible material and carbon nanotube by layer-by-layer self-assembly technique Electrochimica Acta 53 (2008) 4089-4095.
[22] J.H. Pazur, K. Kleppe, The oxidation of glucose and related compounds by glucose oxidase from Aspergillus niger, Biochemistry, 3 (1964) 578-583.
[23] G. Sauerbrey, Verwendung von Schwingquarzen zur Wägung dünner Schichten und zur Mikrowägung, Z. Phys. 155 (1959) 206-222.
[24] E. Barsoukov, Impedance Spectroscopy. Theory Experiment and Applications, J.R. Macdonald (Ed), 2nd ed., Wiley, New York, 2005
[25] M. M. Barsan, R. C. Carvalho, Y. Zhong, X. L. Sun, and C. M. A. Brett, Carbon nanotube modified carbon cloth electrodes: Characterisation and application as biosensors, Electrochim. Acta, 85 (2012) 203–209.
[26] Analytical Methods Committee, Recommendations for the definition, estimation and use of the detection limit, Analyst, 112 (1987) 199-204.
[27] B.-Y. Wu, S.-H. Hou, M. Yu, X. Qin, S. Li, Q. Chen, Layer-by-layer assemblies of chitosan/multi-wall carbon nanotubes and glucose oxidase for amperometric glucose biosensor applications, Mat. Sci. Eng. 29 (2009) 346-349.
[28] X. Wei, J. Cruz, W. Gorski, Integration of enzymes and electrodes: spectroscopic and electrochemical studies of chitosan-enzyme films, Anal. Chem., 74 (2002) 5039-5046
[29] G. Zeng, Y. Xing, J. Gao, Z. Wang, X. Zhang, Unconventional layer-by-layer assembly of graphene multilayer films for enzyme-based glucose and maltose biosensing, Langmuir 26 (2010) 15022-15026.
[30] J. Liu, N. Kong, A. Li, X. Luo, L. Cui, R. Wang, S. Feng, Graphene bridged enzyme electrodes for glucose biosensing application, Analyst 138 (2013) 2567-2575.
[31] H. Gu, Y. Yu, X. Liu, B. Ni, T. Zhou, G. Shi, Layer-by-layer self-assembly of functionalized graphene nanoplates for glucose sensing in vivo integrated with on-line microdialysis system, Biosens. Bioelectron. 32 (2012) 118-126.
[32] Y.-Q. Zhang, Y.-J. Fan, L. Cheng, L.-L. Fan, Z.-Y. Wang, J.-P. Zhong, L.-N. Wu, X.-C. Shen, Z.-J. Shi, A novel glucose biosensor based on the immobilization of glucose oxidase on layer-by-layer assembly film of copper phthalocyanine functionalized graphene, Electrochim. Acta 104 (2013) 178-184.
[33] H.B. Nguyen, V.C. Nguyen, V.T. Nguyen, T.T.T. Ngo, N.T. Nguyen, T.T.H. Dang, D.L. Tran, P.Q. Do, X.N. Nguyen, X.P. Nguyen, H.K. Phan, N.M. Phan, Graphene patterned polyaniline-based biosensor for glucose detection, Adv. Nat. Sci.: Nanosci. Nanotechnol. 3 (2012) 025011.
[34] J. Hui, J. Cui, G. Xu, S.B. Adeloju, y: Wu Direct electrochemistry of glucose oxidase based on Nafion-graphene-GOD modified gold electrode and application to glucose detection Mater. Lett. 108 (2013) 88-91.

Figure captions

Fig. 1. Gravimetric measurements monitored at an AuQC, central frequency 10 MHz, using a AuQC microbalance (AuQCM): (A) – frequency shift and (B) – mass variation during the LbL self-assembly: (——) $chit^+$(NG+GOx) and (——) $chit^+$(GOx).

Fig. 2. Cyclic voltammetry at **(**– – –) AuQC, (——) AuQC/$chit^+$ and (——) AuQC/$chit^+$/PSS^-/$chit^+$ in 0.1 M NaPB pH 7.0, v = 50 mV s^{-1} for $chit^+$ incorporating (A) NG+GOx and (B) GOx.

Fig. 3. Electrochemical impedance spectra recorded at: (●) AuQC, (▼) AuQC/$chit^+$ and (■) AuQC/$chit^+$/PSS^-/$chit^+$ for $chit^+$ incorporating (A) NG+GOx and (B) GOx, at -0.2 V vs. Ag/AgCl; (C) equivalent circuit used to fit the spectra.

Fig. 4. (A) Fixed potential chronoamperogram recorded at AuQC/$chit^+$(NG+GOx)/PSS^- /$chit^+$(NG+GOx) and (B) corresponding calibration plot; applied potential -0.2 V vs. Ag/AgCl

Tables

Table 1. Equivalent circuit element values obtained by fitting of the impedance spectra from Figure 3 for modified electrodes with chitosan layers chit^{+}(NG+GOx) and chit^{+}(GOx)

Table 2. Comparison of analytical performance of the developed biosensor with some similar ones reported in the literature

Figure 1

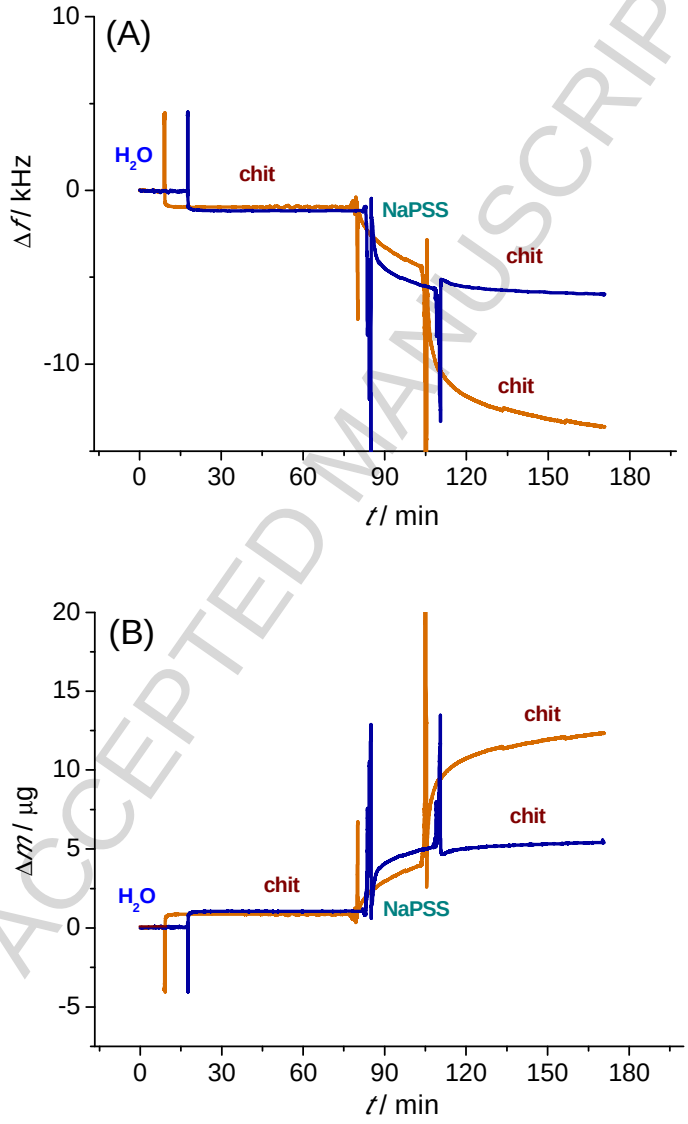

Figure 2

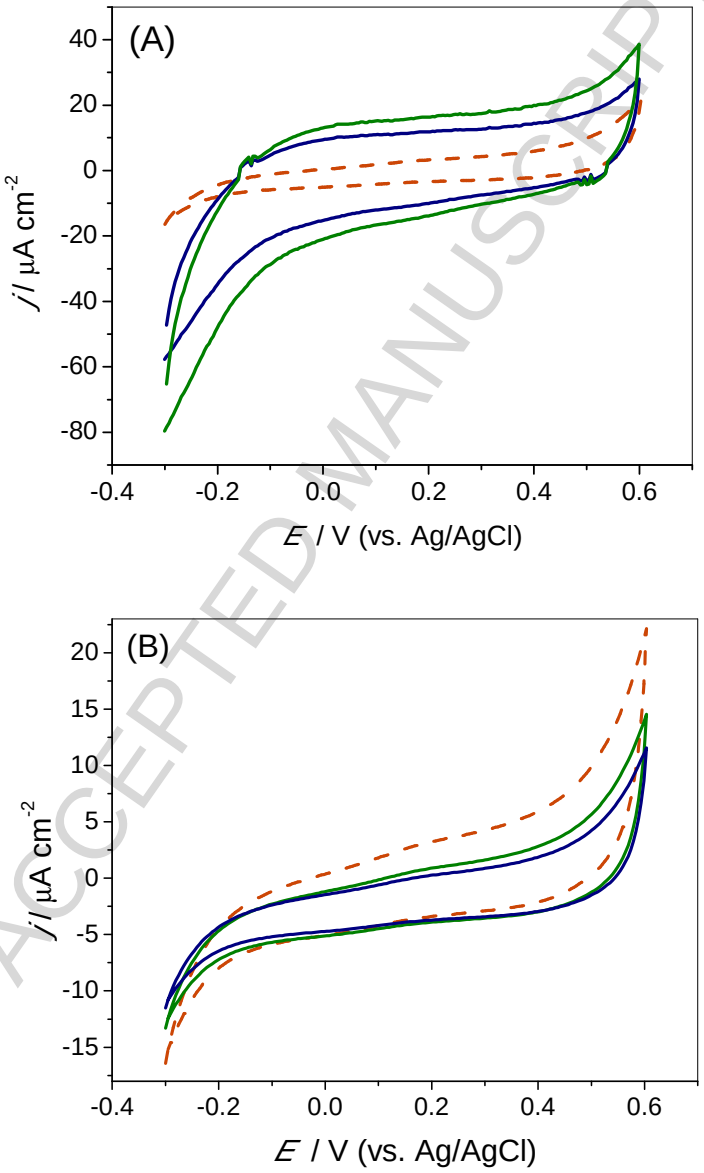

Figure 3

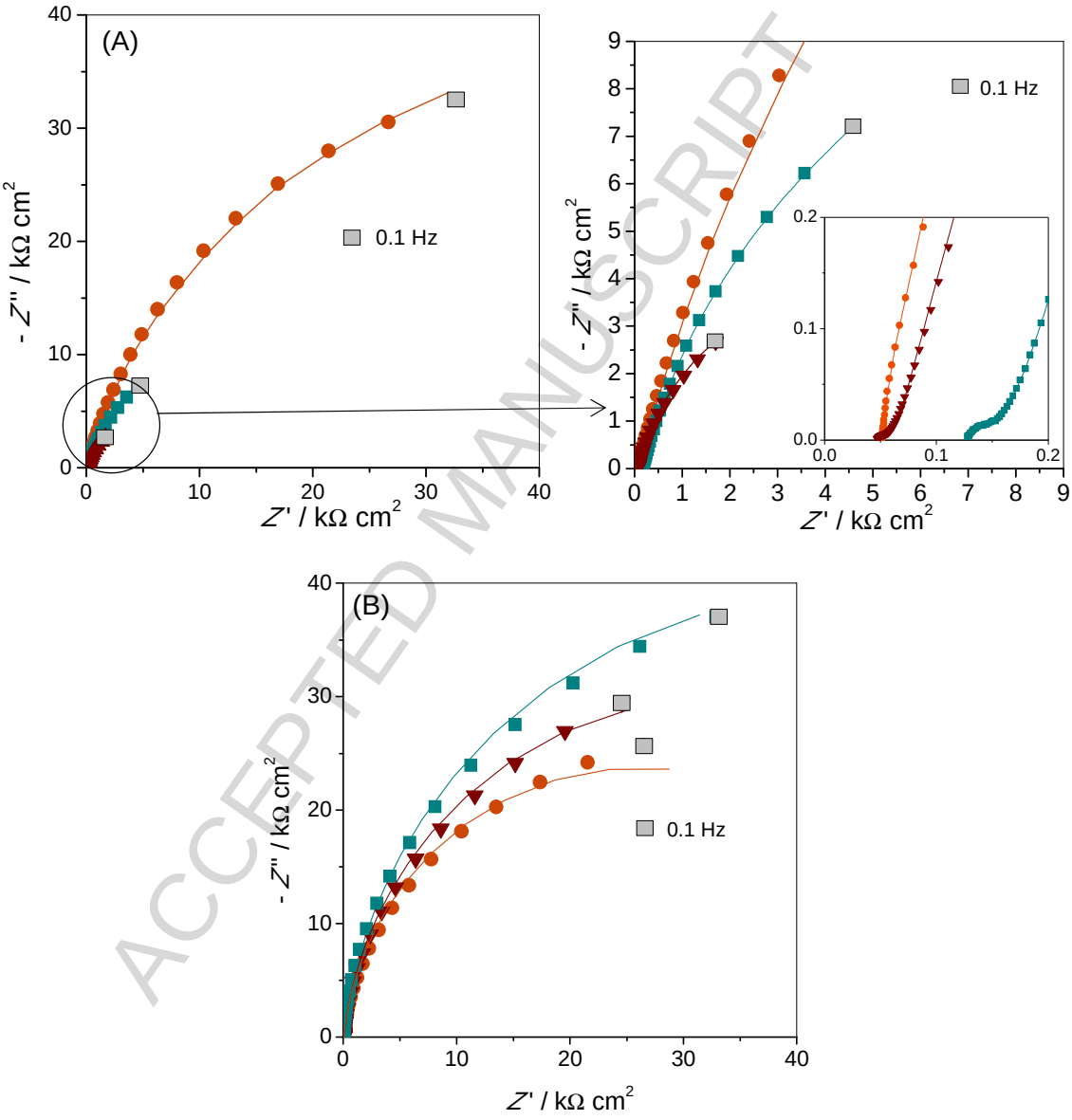

(C)

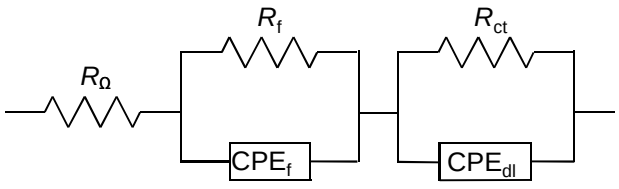

Figure 4

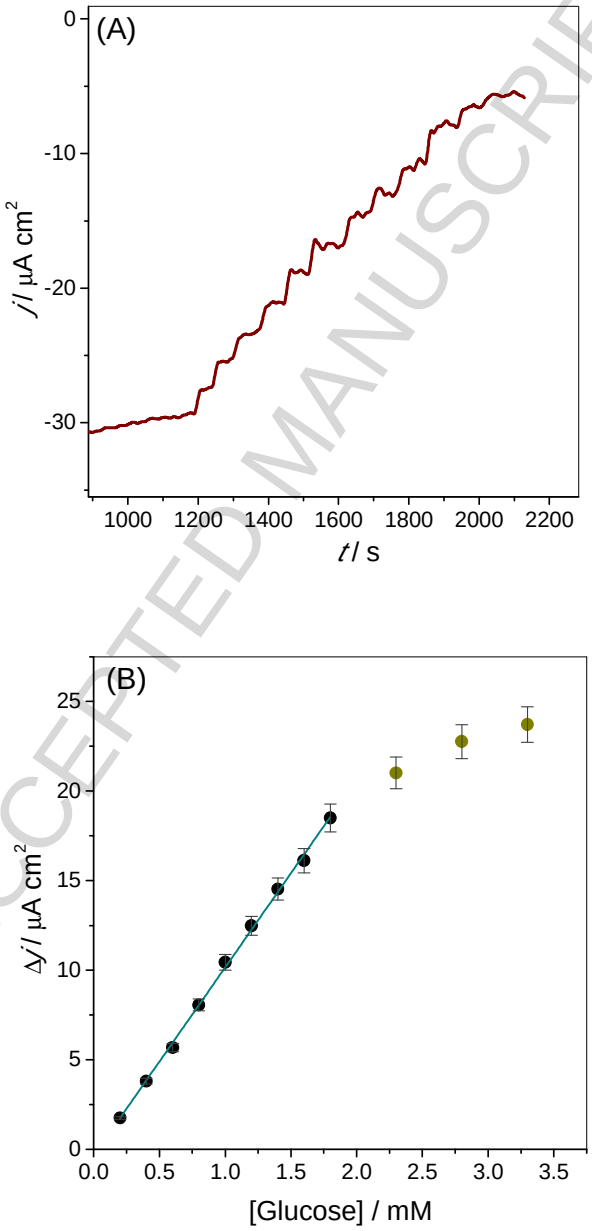

Table 1. Equivalent circuit element values obtained by fitting of the impedance spectra from Figure 3 for modified electrodes with chitosan layers chit$^+$(NG+GOx) and chit$^+$(GOx)

Electrode	R_{ct} / kΩ cm^2	CPE_{dl} / μF cm^{-2} s$^{\alpha-1}$	α_1	R_f / Ω cm^2	CPE_f / mF cm^{-2} s$^{\alpha-1}$	α_2
AuQC	86.9	18.6	0.85	-	-	-
AuQC/chit$^+$(NG+GOx)	8.60	346	0.86	17.8	1.24	0.60
AuQC/chit$^+$(NG+GOx)/PSS$^-$ /chit$^+$(NG+GOx)	23.2	128	0.86	46.3	0.413	0.62
AuQC	52.1	21.1	0.96			
AuQC/chit$^+$(GOx)	65.6	15.6	0.94			
AuQC/chit$^+$(GOx)/PSS$^-$ /chit$^+$(GOx)	86.7	15.6	0.95			

Symbols: AuQC, gold quartz crystal; NG, nitrogen-doped graphene; GOx, glucose oxidase; PSS$^-$, polystyrenesulfonate.

Table 2. Comparison of analytical performance of the developed biosensor with some similar ones reported in the literature.

Biosensor architecture	Technique	*E* / V vs. Ag/AgCl	LoD / µM	Sensitivity/ µA cm^{-2} mM^{-1}	reference
Chit-MWCNT/GCE	Chronoamp.	-0.20	22	28.8	[10]
Graphene–chit/GCE	CV	-0.45	20	37.9	[16]
{Chit/MWCNT/GOx}*n*/PB/ITO	Chronoamp.	0.0	50	8.0	[21]
(GOx/Chit-MWCNTs)$_8$/(PVS/PAA^1)$_3$/Pt	Chronoamp.	+0.60	21	6.3	[27]
Chit-GDI-AY9-GOx/Pt[a]	Chronoamp.	+0.45	10	42.0	[28]
(PEI/PAA^2-graphene)$_3$-(PEI/GOx)$_n$/GCE	Chronoamp.	+0.9	168	0.3	[29]
{GOx/pyrene-graphene}$_n$/GE[b]	CV	+0.28	154	0.6	[30]
{IL-RGO/S-RGO}$_n$/GOx/Nafion/GCE	Chronoamp.	-0.20	3.0	1.0	[31]
GOx/Nafion/(LbL)$_{3.5}$/ABS/GCE	CV	-0.41	50	17.5	[32]
Graphene/Fe_3O_4/PANi/GOx/Pt	Chronoamp.	+0.70	-	47.0	[33]
Nafion-Graphene-GOx/Au	CV	-0.50	40	21.9	[34]
chit$^+$(NG+GOx)/PSS$^-$ /chit$^+$(NG+GOx)/ AuQC	Chronoamp.	-0.20	64	10.5	This work

Symbols. PB, Prussian Blue; ITO, indium tin oxide; PVS, poly(vinyl sulfonate); PAA^1, poly(allylamine); GDI, glutaric dialdehyde; AY9, acetyl yellow 9, PEI, poly(ethyleneimine); PAA^2, poly(acrylic acid); GE, graphite electrode; IL-RGO, amine-terminated ionic liquid - reduced graphite oxide; S-RGO, sulfonated reduced graphite oxide; (LbL)$_{3.5}$, 3.5 bilayers of functionalised graphene (+) and graphene modified with copper phthalocyanines (-); ABS, p-aminobenzenesulfonic acid; PANi, polyaniline.

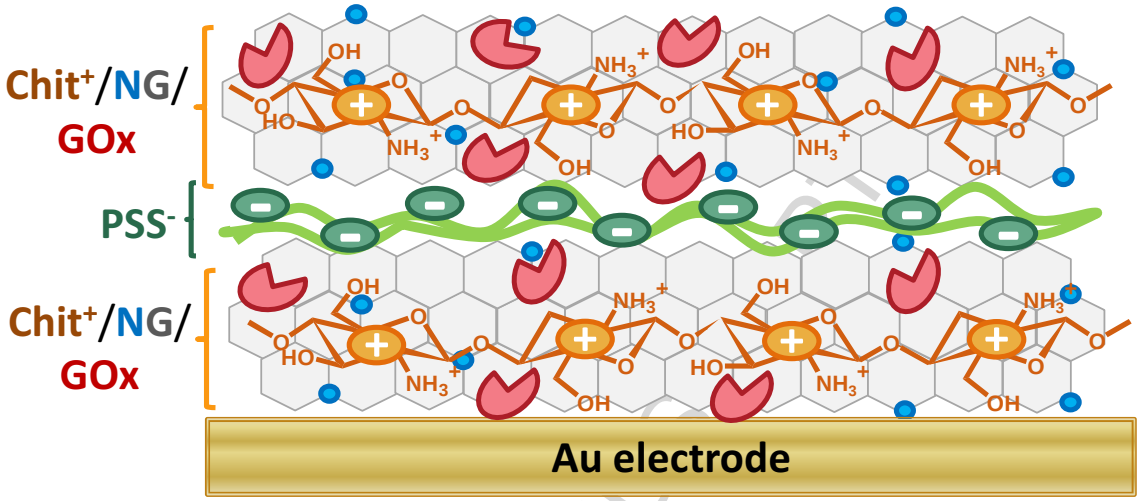

Graphical Abstract

HIGHLIGHTS

- New, very stable self-assembled layer by layer (LbL) enzyme biosensor
- LbL of N-doped graphene/glucose oxidase/chitosan and poly(styrene sulfonate)
- Gravimetric quartz crystal microbalance monitoring of multilayer film formation
- Characterisation by cyclic voltammetry and electrochemical impedance spectroscopy
- The biosensor works at low potential with high sensitivity and operational stability